When Tags 'Read' Each Other: Enabling Low-cost and Convenient Tag Mutual Identification

Haofan Cai*, Ge Wang[†], Xiaofeng Shi*, Junjie Xie[‡], Minmei Wang*, Chen Qian*

* University of California Santa Cruz, CA 95064, USA

[†]Xi'an Jiaotong University, Shanxi Xi'an 710049, P. R. China.

[‡] National University of Defense Technology, Changsha Hunan 410073, China

Abstract—Though being widely used in industrial and logistic applications, current passive RFID technology still has a fundamental limitation: Individual users, who do not carry any reader, are difficult to interact with tagged items, such as retrieving their digital profiles and requesting certain association with them. Recent proposals to improve user-item interaction experience rely on special hardware such as smartphone based RFID scanner. This work presents a promising approach to allow each user to interact with tagged item using only one passive tag, which is named Tag Mutual Identification Interface (TagMii). TagMii requires a user to put her user tag in a physical proximity with an item tag to express certain interactions between the user and item. The key idea behind TagMii is to utilize two experimental observations: 1) inductive coupling for detecting interaction events, and 2) channel similarity for determining the actual interacting tags. We implement TagMii using commodity off-the-shelf RFID devices and conduct experiments in complex environments with rich multipath, mobility, wireless signals, electrical devices, and magnetic fields. The results show that TagMii provides accurate mutual identification. TagMii is a completely new approach for user-item interactions in pervasive environments and enables many user-friendly IoT applications with low cost and convenience.

I. INTRODUCTION

The Radio Frequency IDentification (RFID) technology, widely considered as a cheap, energy-efficient, and scalability solution of the Internet of Things (IoT), has been deployed for ubiquitous applications, such as retailing, warehouse, transportation, and manufactures. The basic functions of RFID that have been extensively studied including: 1) Collect the identity information of tagged items or users in a target area [1]; 2) Count or estimate the population of items/users [2]–[4]; 3) Advanced sensing tasks that explore the physical signal features of RFID, such as localization and tracking [5]–[15], and human activity sensing [16]–[19].

However, current passive RFID applications are mainly restricted to industrial and logistic areas, due to an *fundamental limitation*: an individual user is difficult to interact with tagged items or other tagged users, if she carries no reader. The interactions with tagged items may include 1) collecting certain information from the digital profile behind a tag, such as the item name, price (for merchandise), packing location and time (for packages); 2) requesting the backend system to connect the user profile with the item profile and conduct certain processing, such as charging this item to the

user account. Hence passive RFID is seldom used in consumer applications.

Recent efforts have been made to improve the consumer-experience of interacting with passive tags, such as small reader [20], smart-phone based RFID scanner [21], and reading tags through the smartphone WiFi interface [22]. Also smartphones may have NFC interfaces. However these methods still require non-trivial hardware carried by the users – a smartphone at a minimum. As a result, children, some seniors, people with certain disabilities, and other people who are not familiar of operating smartphones cannot utilize these methods.

This work provides an extremely low-cost and convenient solution for user-tag interaction by answering this questions: Can a user initiate the interaction with tagged items with nothing but a single passive tag? The proposed solution is called TagMii (Tag Mutual Identification Interface). TagMii allows two tags 'read' each other: If two tags are placed in a close physical proximity, the reader can identify these interacting tags among many other tags in the environment. The two tags can be the identifiers of a user and an item, or two users. We present a number of IoT applications that can utilize TagMii to perform simple yet important tasks, which was difficult to achieve in existing RFID systems:

Application 1. A museum displays a collection of artworks. A tag is placed on the wall next to each artwork. Each user wears a set of wireless headphones. If a user wants to listen to the commentary of an artwork, she puts her user tag close to the tag of the artwork. The backend system then sends the recorded commentary to her headphones in the preferred language according to the user profile.

Application 2. In a cashier-free retail store, a tag is attached to each type of items. When a user puts her user tag close to an item tag, she can hear the item price, description, and reviews from her headphones. She may repeat this operation to request the backend system to put the item in her virtual shopping cart, which can be later charged by warehouse workers.

Application 3. In a smart home, each appliance can be controlled by interacting one or more tags next to it. TagMii allows the backend system to verify the identity of the user tag. For example, the thermostat can only be controlled by family members.

Application 4. In a conference, two attendees chatting

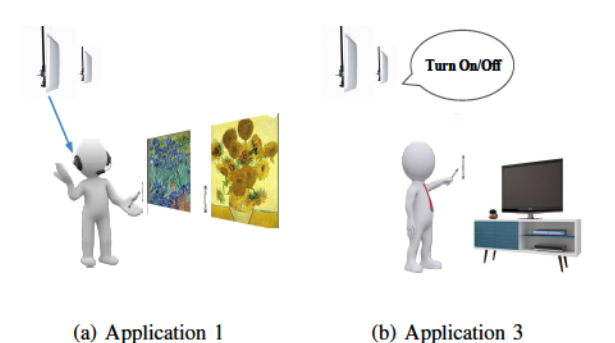


Fig. 1. Two applications of TagMii

during a coffee break may put their user tags together. An app running in the backend system will automatically exchange their digital profile (e-business card) and record the time and location. After the conference, the collected digital profiles will be emailed to the user and she can easily review the profiles from the attendees who she has chatted to.

Some existing technologies may also be able to accomplish the tasks in the above applications. For example, a customer can use her smartphone to scan the barcode [23] or QR code [24] attached to the items to retrieve the item information and/or request the payment. Some mobile apps support ebusiness card exchange. Compared to these solutions, the key advantage of TagMii is that it is smartphone-free and hence very convenient for children, some seniors, people with certain disabilities, and others who do not operate smartphones. Other advantages of TagMii include: 1) Easy to carry. The user tag can be attached to a conference badge (or museum badge, shopping badge in a similar design).2) Fast interaction. Using smartphones for code scanning or profile exchange usually takes half a minute. TagMii may only take 10 seconds. Such speed advantage is especially important in busy situations like conference breaks. 3) TagMii does not require light conditions compared to code scanning, suitable for museums and warehouses. 4) System manager can easily obtain the useful information monitored by the backend, such as the popular goods, shopping habits of users, and preference of artworks by users with different ages and regions. One might notice that TagMii still requires a reader placed in each room. However this method is scalable: one reader per room can monitor multiple user tags and item tags.

The design of TagMii is based on two important ideas: inductive coupling and phase profile similarity. We observed from experiments that when two tags are placed in physical proximity (e.g., < 2cm), the backscatter signal from either tag would be different from the signal by putting the tag alone, called the *inductive coupling state*. A sudden change of the backscatter signal strength from both tags will occur at the beginning of inductive coupling. TagMii tracks such signal strength change to find out the potential tags that may be in the coupling state, among all tags in the environment. In addition, to further select the pair of tags that are truly in the coupling state, we utilize the tags' *phase profiles* collected by multiple antennas based on the fact that nearby RFID tags experience a

similar multipath environments and thus exhibit similar phase profiles. By evaluating the similarities between phase profile of potential coupling tags, TagMii can accurately identify the tags placed together and therefore recognize the user and the target item that is interacting with her.

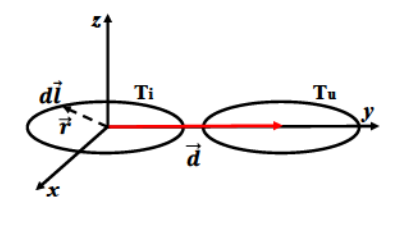
In this work, we address and resolve three main challenges in design and implementation of TagMii. 1) We design accurate tag coupling detection algorithm for **complex environments with rich multipath, mobility, wireless signals, electrical devices, and magnetic fields**. 2) TagMii should identify the coupling tags in a short time even though there are a large number of tags in the environment. 3) TagMii should be able to extract sufficient information from signal dynamics using commodity RFID readers, which have low measurement resolution.

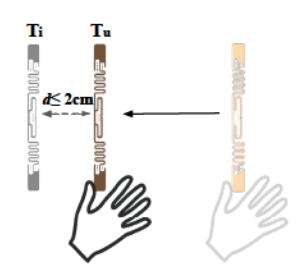
We implement TagMii using commodity off-the-shelf (COT-S) RFID devices only. Although we are the first to study mutual identification (interacting a tag with another tag), we do *not* conduct our study in a laboratory condition that is free of multipath reflectors and moving objects. In fact, all implementation and experiments are conducted in various complex environments with rich multipath, mobility, wireless signals, electrical devices, and magnetic fields, in order to valid TagMii for practical applications. Even in these environments, TagMii provides high accuracy. We believe TagMii serves as an important extension of current RFID applications and tag mutual identification will attract further research due to its low-cost and convenience to enable consumer experience of interacting with tagged items.

The remaining paper is organized as follows. Section II presents the related work. Section III introduces the background and models. We present the detailed design of TagMii in Section IV. We show the system implementation and evaluation results in Section V. We provide some discussion in Section VI and conclude this work in Section VII.

II. RELATED WORK

User-item interaction: Automatic identification and data capture (AIDC) techniques like barcodes [23] and quick response (QR) codes [25] provide fast, easy and accurate data collection approaches for inventory control, product management [26]. A barcode or QR code requires to be read by a scanner or camera. Different from them, RFID does not require such line-of-sight scanning as RF signals can penetrate through non-metal objects [24]. RFID sensing techniques have been widely used for detecting the gesture-based inputs [27], [28]. IDSense [29] recognizes the physical movements and touch events of everyday objects using real-time classification of the RSSI and phase angles with only one reader, however, it requires training and calibration and is insufficiently precise. PaperID [30] is a similar work that uses supervised machine learning to detect different types of on-tag and free-air interactions with custom-designed RFID tags. And Pradhan et al. [31] show how changes in the received signal phase caused by touching on RFID tag can be leveraged to detect the finger swipe or touch gesture without any pre-training stage. There





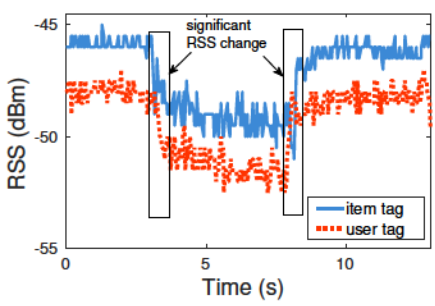


Fig. 2. Model of two coupling tags

Fig. 3. Inductive coupling

Fig. 4. Signal strength change of two coupling tags

also exists a research direction trying to solve the issue that users have to use RFID readers to query tags, and thus, cannot benefit from the convenience provided by their mobile devices. TiFi [22] allows a 2.4 GHz WiFi receiver to identify 800 MHz UHF RFID tags. Other related techniques include small RFID reader [20] and smart-phone based RFID scanner [21]. Compared with these works, TagMii only requires each user to carry a tag and/or other necessary feedback devices of the application (such as headphones in the museum commentary case).

RFID Localization: Using RFID for Localization is a possible research direction for TagMii, considering any two tags in very close positions are interacting tags. Early RFIDbased localization methods mainly rely on RSSI information to acquire tag location. They usually rely on densely predeploying tags in the area of monitoring and leverage the precollected RSSI values of these tags as references to locate a specific tag [5], [32], [33]. The major limitation of RSSIbased methods is that they are highly sensitive to multipath propagation, and thus can not achieve high-accuracy localization in multi-path environment. Meanwhile, there is a growing interest in using phase differences [9], [28], [34], [35] or Angle of Arrival(AoA) information [8] to estimate absolute locations of tags. [Localization using advanced electromagnetism and communication techniques like synthetic aperture radar (SAR) [36] or multiple antennas [10] have also been studied. However, simply adopting the existing RFID tag localization protocols [8]-[10], [36] to localize all tags in TagMii will not work, as existing tag localization methods using commodity readers are not able to achieve location errors < 10cm [9], [10]. Hence it is likely that two tags within 10-20cm distance are localized to a same position. These tags are not necessarily the user tag and item tag that are interacting.

III. BACKGROUND AND MODEL

A. Problem specification

TagMii targets on making convenient user-item interaction using RFID tags. In TagMii, we employ two types of tags, the first type are called *user tags* and the other are *item tags*. Each user registered to TagMii holds a user tag, and each item (or each type of items) in the application is labeled by an item tag. When a user wants to interact an item, she puts her user tag in a close distance (< 2cm) to the corresponding item tag.

TagMii can be completely implemented with COTS RFID devices. It requires *no modification* on current RFID tag or

reader hardware. It is implemented as a software program on the backend server connected to the reader, which stores the profile information of all users and tags that could appear in the system. TagMii analyzes the physical-layer signals collected by the reader antennas from all tags in the environments and determines the interacting ones.

B. Basic ideas

TagMii is based on two important facts and observations from practical RFID communication: inductive coupling and channel similarity. If two tags are put in a physical proximity, they will interfere with each other and cause changes on their backscatter signals. This phenomenon is called inductive coupling [37] [38]. Our key innovative idea is to use the occurrence of the coupling phenomenon as an indicator of user-tag interaction, which can be detected by analyzing the signals collected by the reader. One additional challenge is that, when users are moving their bodies to 'scan' the item tags using their user tags, the body movement may cause signal changes on other tags in the environments that are not involved in this interaction. By monitoring the signal variations, we can find out a list of tags called candidate tags that may be coupling with the user tag. To figure out which candidate tag is indeed the target tag that is being read by the user, TagMii further uses the *channel similarity* between the user tag and those candidate tags. Channel similarity is based on the observation that two coupling tags will show high similarity on their received phase information. In fact, the wireless channel is determined by a series of factors, including tags' locations, outside environment, and moving objects. Only the target tag, which actually has a close distance with the user tag will experience similar communication channels and shows high similarity on their received signal phases.

C. Inductive coupling

In the environment, we may have dozens of or even hundreds of tags that represent different items and people. Each of them may be the one that the user is interacting. It is extremely time-consuming and compute-intensive for our system to compare all the tags' signals with that of the user tag. Fortunately, we observe that when the user tag is close to the item tag, there is a sudden decrease on both of their received signal strength (RSS) [39]. We specify this phenomenon with both theoretical model and practical experiments.

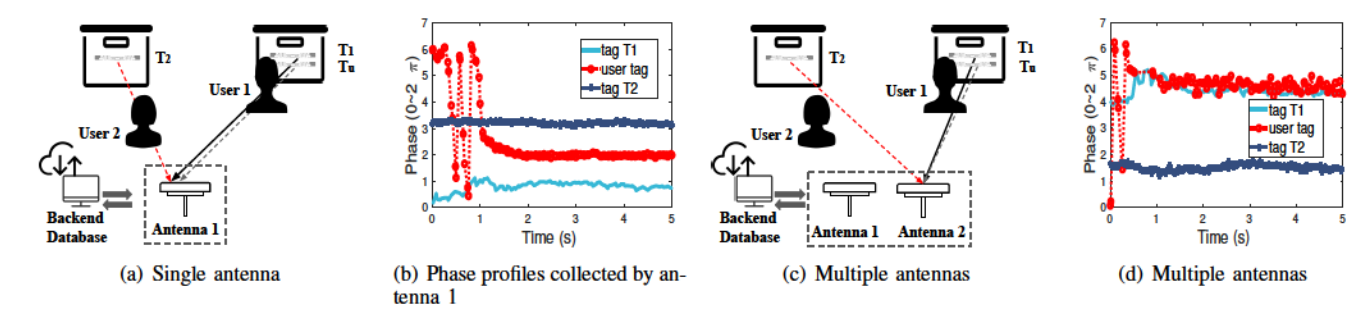


Fig. 5. Phase profiles and differences captured by multiple antennas

In theory, a passive RFID tag can be modeled as a circular loop. If there is no user tag, for each item tag T_i , a steady current I_i will be induced by the electronic waves send by the RFID reader. After transmitting in the wireless channel, which has a channel parameter of $h_{t\leftrightarrow R}$, the received signal strength RSS_i of the tag T_i should be:

$$RSS_i = h_{t \leftrightarrow R} \cdot 10 \cdot loq_{10}(1000 \cdot P_i), \tag{1}$$

where P_i is the power of tag T_i and U is the voltage only related to the reader's signals:

$$P_i = I_i \cdot U. \tag{2}$$

However, when a user tag is placed close enough (Fig. 3), *i.e.*, 2cm away from the item tag, the RSSes of the two tags will significantly change. As shown in Fig. 2, the user tag and the item tag can be modeled as two circular loops, whose radius vectors are \overrightarrow{r} . Let vector \overrightarrow{d} denotes the directional vector from the center of item tag's circular to that of the user tag. Once the RFID reader sends an electronic signal, it will induce a steady current of I_i to tag T_i . The steady current will generate a magnetic field around it. The mutual inductance M between item tag T_i and the user tag T_u can be calculated by:

$$M = \frac{\mu_0}{4\pi} \oint_c \frac{1}{|\vec{d} - \vec{r}|^2}.$$
 (3)

Due to the influence of the magnetic field, the current I_u in tag T_u changes to I'_u :

$$I_u' = I_u - \frac{1}{R_u} \cdot \frac{dM}{dt} \cdot I_i,\tag{4}$$

where R_u is the resistance of user tag T_u . Observing Eq. 4 and 3, we find that both the resistance R_u and mutual inductance M are positive values. In other words, we have a conclusion that:

$$I_u' < I_u \tag{5}$$

The situation is similar for the item tag T_i , i.e. $I_i' < I_i$. In other words, for a stable channel, the received signal strength RSS_i and RSS_u for these two tags will decrease due to the inductive coupling.

We also conduct a set of experiments to verify the modelling results. We first put one tag T_u in Fig. 3 with a distance of 2cm from a static tag T_i . After keeping the two tags stable for two seconds, we take away tag T_u . The signals of the two tags are shown in Fig. 4. Obviously, due to inductive coupling, both

tags experience significant decreases on their RSSes when they are putting together. During the coupling their RSSes keep a lower values than those before and after.

By observing the sharp and simultaneous decreases of their RSSes, TagMii can find out a few candidate tags, whose population is much smaller than the entire set of tags. Then finding the actually coupling tags from the candidate tags is much easier and time-efficient. In Section IV, we will specify the detailed algorithm to select the candidate tags.

D. Channel similarity

In fact, only observing the decrease of the RSS can help to select the candidate tags but may not exactly figure out the actual coupling tags. That is because the RSSes of the other tags will also be influenced by the user movement and environmental dynamics. If a moving object blocks the line-of-sight (LOS) propagation path between a tag and the reader antenna, the tag's RSS will also experience a decrease. In addition, if multiple users are using their user tags to scan different item tags, all of the involving tags will fall in the coupling state with RSS decrease. To resolve this problem, we further compare the phase data of the candidate tags. The basic idea behind this is based on the channel similarity of two tags in a physical proximity.

Actually, besides the phase changes over distance, the measured phase θ_{ij} of tag T_i at antenna A_j also contains the initial phase of the tag and the antenna, i.e., θ_{T_i} and θ_{A_j} , respectively. We can represent θ_{ij} as follows:

$$\theta_{ij} = (\theta_{d_{ij}} + \theta_{m_{ij}} + \theta_{T_i} + \theta_{A_j}) \mod 2\pi, \tag{6}$$

where $\theta_{d_{ij}}$ is the phase changes over distance and $\theta_{m_{ij}}$ represents the phase changes introduced by the multi-path effects. As we know, the tag's phase changes over distance can be calculated as:

$$\theta_{d_{ij}} = 2\pi \left(\frac{2d_{ij}}{\lambda}\right) \mod(2\pi),\tag{7}$$

where d_{ij} is the LOS distance between tag T_i and antenna A_j . Observing Eq. 6, we find that the received phase is not only determined by the distance and the outside environment, but also impacted by device diversity. Even if two different tags are very close with each other, i.e., have similar θ_d and θ_m , their measured phases are high likely to be different with each other. To deal with the errors introduced by device diversities, we employ multiple antennas in our system (Fig.5). The main

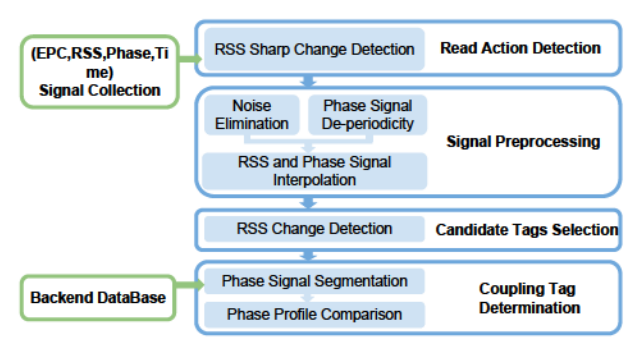


Fig. 6. System Overview

idea is that even though different tags have ambiguous and diverse initial phases, such difference can be cancelled using the measurement from two antennas. We calculate difference of the phases of tag T_i that collected at antennas A_1 and A_2 :

$$\Delta\theta_i = \theta_{i1} - \theta_{i2} = (\theta_{d_{i1}} - \theta_{d_{i2}}) + (\theta_{m_{i1}} - \theta_{m_{i2}}) + (\theta_{A_1} - \theta_{A_2}). \tag{8}$$

In this way, the tag diversity can be cancelled. For a user tag T_{n} and an item tag T_i that are very close to each other, their LOS path are very similar (the path difference is much less than the LOS propagation path), i.e., $\theta_{d_{uj}} \approx \theta_{d_{ij}}$. Existing work [40] demonstrates that the channel conditions are extremely similar for two tags in physical proximity. Hence we may use the similarity among the phase changes to infer the two coupling tags, i.e., $\theta_{m_{uj}} \approx \theta_{m_{ij}}$. The antenna difference $(\theta_{A_1} - \theta_{A_2})$ is a constant for all the tags. As a result, the phase difference $\Delta \theta_i$ of the target item tag should be close to that of the user tag, i.e., $\Delta \theta_u$. On the other hand, other candidate tags, though have a decrease on their RSSes, are likely to have different LOS distances and multipath effects with the user tag, and hence their phase difference $\Delta\theta_i$ would have a much larger gap with that of the user tag, namely $\Delta \theta_u$. By comparing the phase differences, we can further determine the target tag among all candidate tags. In Section IV, we will specify more details of the algorithm to determine the coupling tags.

IV. SYSTEM DESIGN

The TagMii program has four modules, namely tag interaction detection, signal preprocessing, candidate tag selection and target tag determination, which are illustrated in Fig. 6. Tag interaction detection determines the begin and end time for an interaction action performed by user. The signal preprocessing module performs RSS profile smoothing and phase de-periodicity over the received signal. Then TagMii selects candidate tags by detecting the RSS decreases and finally determines the interacting tags among all the candidate tags by comparing the phase profiles.

A. Detect the action of interaction

When a user holds up the user tag to place it together with a target item tag, the hand movement will result in an abrupt change in the RSS of user tag (shown in Fig.7(a)). TagMii also requests that the user waves the user tag slightly in purpose to make this signal change more obviously if the user wants to improve the detection accuracy. TagMii can leverages these

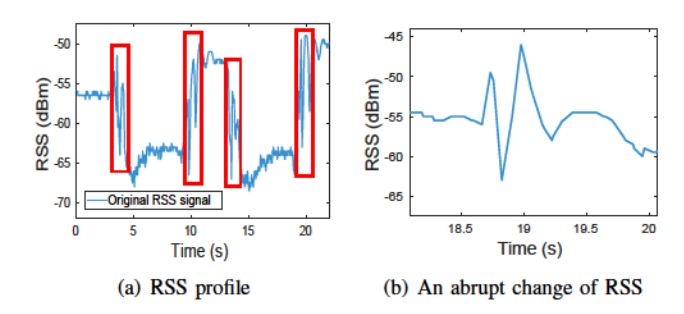


Fig. 7. RSS profile of user tag for two interactions

time points with RSS discontinuity to locate the starting and finishing time for tag interaction. TagMii uses a threshold R_h to detect interaction events:if the RSS difference between current and following signal points is larger than R_h , then the timestamp of this signal point is considered as potential starting/finishing time for tag interaction.

After locating these time points, TagMii can leverage the aforementioned inductive coupling phenomenon to determine whether the current moment is the starting time for tag interaction. If the user does begin to interact an item tag, then the RSS will experience a significant decrease.

B. Signal Preprocessing

Before feeding the received data into the TagMii algorithms, preprocessing is necessary for a better performance. As shown in Fig. 6,there are three steps in the signal preprocessing module, namely RSS profile smoothing, phase de-periodicity, and RSS and phase profile interpolation.

RSS profile smoothing: We require TagMii to use commercial RFID devices, which have low resolution on the RSS measurement compared to advanced devices such as the software defined radio. The minimum RSS resolution is 0.5dB by using the ImpinJ R420 reader [21], which is far from sufficient for accurately capturing necessary tag signal changes. As shown in Fig. 8, the raw RSS profile (blue line) is fluctuate and noisy, which is error-prone for the following signal processing. To address this problem, we first smooth the raw RSS profile by employing a low-pass filter. Keep in mind that the RSS variations introduced by inductive coupling has a much lower frequency compared to the Gaussian white noise produced by electronic devices, we choose an appropriate lowpass filter and the performance are shown as the red dot line in Fig. 8. Obviously, it removes a lot of fluctuations and make the signal trend more clear. However, the low-pass filter may also obscure the exact change time point of the raw RSS profile. So in the candidate tag selection, we propose to employ a small window to locate the RSS change point.

Phase de-periodicity: The raw phase data is a periodic value ranging from 0 to 2π , which will change gradually. However we may observe that the raw phase data show sharp decreases or increases. We named this phenomenon as 'faked changes'. Due to the movement caused by human beings or other objects, the phases may vary all the time. We should tell the difference between the faked changes from the true phase

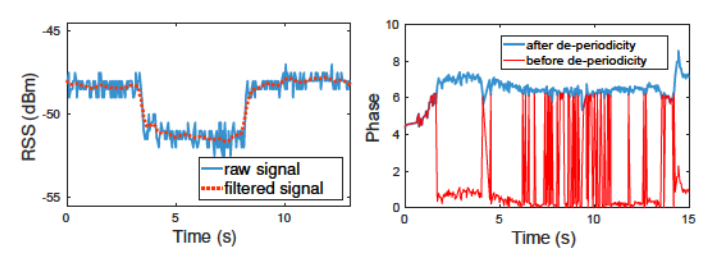


Fig. 8. RSS signal noise elmination

Fig. 9. Phase signal de-periodicity

changes, and only remove the former one. We propose to find the fake changes that are sharp and the true changes that are more gradual, among the sampling data. To recognize the fake changes, we add or subtract an additional 2π to the following received phases, *i.e.*:

$$\theta(t+1,t_e) = \begin{cases} \theta(t+1,t_e) - 2\pi, & \theta(t+1) - \theta(t) > (2-\epsilon_\theta) \cdot \pi \\ \theta(t+1,t_e) + 2\pi, & \theta(t+1) - \theta(t) < (\epsilon_\theta - 2) \cdot \pi \\ \theta(t+1,t_e) + 2\pi, & \theta(t+1) - \theta(t) < (\epsilon_\theta - 2) \cdot \pi \\ \theta(t+1,t_e) + 2\pi, & \theta(t+1) - \theta(t) < (\epsilon_\theta - 2) \cdot \pi \\ \theta(t+1,t_e) + 2\pi, & \theta(t+1) - \theta(t) < (\epsilon_\theta - 2) \cdot \pi \\ \theta(t+1,t_e) + 2\pi, & \theta(t+1) - \theta(t) < (\epsilon_\theta - 2) \cdot \pi \\ \theta(t+1,t_e) + 2\pi, & \theta(t+1) - \theta(t) < (\epsilon_\theta - 2) \cdot \pi \\ \theta(t+1,t_e) + 2\pi, & \theta(t+1) - \theta(t) < (\epsilon_\theta - 2) \cdot \pi \\ \theta(t+1,t_e) + 2\pi, & \theta(t+1) - \theta(t) < (\epsilon_\theta - 2) \cdot \pi \\ \theta(t+1,t_e) + 2\pi, & \theta(t+1) - \theta(t) < (\epsilon_\theta - 2) \cdot \pi \\ \theta(t+1,t_e) + 2\pi, & \theta(t+1) - \theta(t) < (\epsilon_\theta - 2) \cdot \pi \\ \theta(t+1,t_e) + 2\pi, & \theta(t+1) - \theta(t) < (\epsilon_\theta - 2) \cdot \pi \\ \theta(t+1,t_e) + 2\pi, & \theta(t+1) - \theta(t) < (\epsilon_\theta - 2) \cdot \pi \\ \theta(t+1,t_e) + 2\pi, & \theta(t+1) - \theta(t) < (\epsilon_\theta - 2) \cdot \pi \\ \theta(t+1,t_e) + 2\pi, & \theta(t+1) - \theta(t) < (\epsilon_\theta - 2) \cdot \pi \\ \theta(t+1,t_e) + 2\pi, & \theta(t+1) - \theta(t) < (\epsilon_\theta - 2) \cdot \pi \\ \theta(t+1,t_e) + 2\pi, & \theta(t+1) - \theta(t) < (\epsilon_\theta - 2) \cdot \pi \\ \theta(t+1,t_e) + 2\pi, & \theta(t+1) - \theta(t) < (\epsilon_\theta - 2) \cdot \pi \\ \theta(t+1,t_e) + 2\pi, & \theta(t+1) - \theta(t) < (\epsilon_\theta - 2) \cdot \pi \\ \theta(t+1,t_e) + 2\pi, & \theta(t+1) - \theta(t) < (\epsilon_\theta - 2) \cdot \pi \\ \theta(t+1,t_e) + 2\pi, & \theta(t+1) - \theta(t) < (\epsilon_\theta - 2) \cdot \pi \\ \theta(t+1,t_e) + 2\pi, & \theta(t+1) - \theta(t) < (\epsilon_\theta - 2) \cdot \pi \\ \theta(t+1,t_e) + 2\pi, & \theta(t+1) - \theta(t) < (\epsilon_\theta - 2) \cdot \pi \\ \theta(t+1,t_e) + 2\pi, & \theta(t+1) - \theta(t) < (\epsilon_\theta - 2) \cdot \pi \\ \theta(t+1,t_e) + 2\pi, & \theta(t+1) - \theta(t) < (\epsilon_\theta - 2) \cdot \pi \\ \theta(t+1,t_e) + 2\pi, & \theta(t+1) - \theta(t) < (\epsilon_\theta - 2) \cdot \pi \\ \theta(t+1,t_e) + 2\pi, & \theta(t+1) - \theta(t) < (\epsilon_\theta - 2) \cdot \pi \\ \theta(t+1,t_e) + 2\pi, & \theta(t+1) - \theta(t) < (\epsilon_\theta - 2) \cdot \pi \\ \theta(t+1,t_e) + 2\pi, & \theta(t+1) - \theta(t) < (\epsilon_\theta - 2) \cdot \pi \\ \theta(t+1,t_e) + 2\pi, & \theta(t+1) - \theta(t) < (\epsilon_\theta - 2) \cdot \pi \\ \theta(t+1,t_e) + 2\pi, & \theta(t+1) - \theta(t) < (\epsilon_\theta - 2) \cdot \pi \\ \theta(t+1,t_e) + 2\pi, & \theta(t+1) - \theta(t) < (\epsilon_\theta - 2) \cdot \pi \\ \theta(t+1,t_e) + 2\pi, & \theta(t+1) - \theta(t) < (\epsilon_\theta - 2) \cdot \pi \\ \theta(t+1,t_e) + 2\pi, & \theta(t+1) - \theta(t) < (\epsilon_\theta - 2) \cdot \pi \\ \theta(t+1,t_e) + 2\pi, & \theta(t+1) - \theta(t) < (\epsilon_\theta - 2) \cdot \pi \\ \theta(t+1,t_e) + 2\pi, & \theta(t+1) - \theta(t) < (\epsilon_\theta - 2) \cdot \pi \\ \theta(t+1,t_e) + 2\pi, & \theta(t+1) - \theta(t) < (\epsilon_\theta - 2) \cdot \pi \\ \theta(t+1,t_e) + 2\pi, & \theta(t+1) - \theta(t) < (\epsilon_\theta - 2) \cdot \pi \\ \theta(t+1,t_e) + 2\pi, & \theta(t+1) - \theta(t) < (\epsilon_\theta - 2) \cdot \pi \\ \theta(t+1,t_e) + 2\pi, & \theta(t+1) - \theta(t) < (\epsilon_\theta -$$

where $\theta(t+1,t_e)$ represents the phase values from time point t+1 to the end time point t_e . ϵ_{θ} is an experimentally-chosen threshold. The performance of phase de-periodicity can be found in Fig. 9, which shows that TagMii can successfully remove the fake changes from the received phase data.

RSS and Phase signal interpolation: According to the ALOHA-based RFID protocol [41], the sample rate for each tag could be highly different. For simply comparing their RSS and phase profiles, we adopt a cubic spline interpolation method to re-sample the RSS and phase sequence with a uniform sampling rate. After this step, TagMii obtains the same number of samples for the tags that are under comparison in a given time period.

C. Candidate Tags Selection

As mentioned in Section III-C, we observe that when the user puts her user tag close to an item tag, both tags will show a significant decreases on their RSS profiles. The coupling user tag can be detected using the method presented in Section IV-A. Here to present the method to select the candidate tags that **might** be coupling with the user tag. If there are multiple user tags that are detected to have coupling, TagMii computes a set of candidates for every user tag using the same method.

The main idea of the tag selection algorithm is to locate every change points in the RSS profile of each item tag and user tag. Since TagMii has obtained the moment when the user tag starts to be in coupling in Section IV-A, if an item tag has experienced a significant RSS change at a similar time as the user tag, we will add this item tag into the candidate tag set S_u of the user tag T_u .

Due to the poor resolution of RSS measurement collected be a COTS reader, locating the exact change point of the smoothed RSS profile is error-prone. In addition, the changing time points for the user tag and the item tag may not align perfectly. To make our algorithm more tolerant to the practical cases, we adopt a sliding window whose size is T and step is Δt . If there is a significant change occurs in the sliding window, we will record the start time of the current window as the changing time point.

However, as aforementioned, many other factors, such as blocking LOS by moving objects, can also introduce an RSS changes. Only one tag in the candidate set is the correct coupling tag. To reduce the number of candidate tags we choose in mistake, we consider the RSS changes of both antennas. That is inspired by a simple but effective idea, the RSS changes effected by the inductive coupling are simultaneously captured by the two antennas. While for the tags that blocked by moving objects, the RSS decreases may not be observed by both antennas – in most cases, the moving objects will not block the LOS from all antennas. Hence we only consider the tags that have significant and simultaneous RSS changes in both antennas and select them as the candidate tags.

Fig. 10 shows an example demonstrating the feasibility of faulti-antenna solution. In this example, a 3×3 tag array (namely tag 01-09) is attached on the wall in an office. The distance between each tag and its neighbor is 40cm. A volunteer is asked to browse the tag array and use the user tag T_u to scan the item T_2 he's interested in at about 4-th second. The scanning behavior will last for about 5s till the user leaves away. During the whole process, RSS profile of each tag-antenna link is collected to explore their temporal dynamics. Fig. 11 plots the some of the RSS measurements in this study. In accordance with our analysis, during the first 10 seconds, the RSS profiles of some tags (T_1) maintain in a relatively stable level, while the RSS trends of T_2, T_3 changes significantly, indicating that the user appoarches the items and impacts these tags's LOS paths sequentially.

D. Coupling Tag Determination

From Section III-B we know that for tag i in the TagMii system, its phase profile at antenna j can be modeled as Eq. 6. If we compare the phase profiles for tag i received at multiple antennas (antennas A_1 and A_2 in our example), we can eliminate the phase shift introduced by the tag hardware or environment.

Based on Eq. 8, if tag i and j are located in a physical proximity, they should have similar values between $\theta_{d_{i1}} - \theta_{d_{i2}}$ and $\theta_{d_{j1}} - \theta_{d_{j2}}$, $\theta_{m_{i1}} - \theta_{m_{i2}}$ and $\theta_{m_{j1}} - \theta_{m_{j2}}$, as well as $\theta_{m_{i1}} - \theta_{m_{i2}}$ and $\theta_{m_{j1}} - \theta_{m_{j2}}$. Hence for samples at any time point $\Delta\theta_i$ should be a small value. We define the *phase difference profile* D_i as a vector where each element is $\Delta\theta_i(T)$ at time T. During the coupling state, D_i and D_j for two tags i and j should be similar. We define an effective distance metric $Dist(D_i, D_u)$ as the Euclidean distance between D_i and D_j to evaluate their similarity.

The coupling tag determination algorithm first computes the phase difference profile D_i for each tag i. TagMii measures the similarities between profiles over a time window with fixed size T. The choice of T determines the latency and processing overhead of computation. Once TagMii has determined the set of candidate tags S_c , it immediately begins measuring the similarities between phase difference profiles over these candidate tags and user tag.

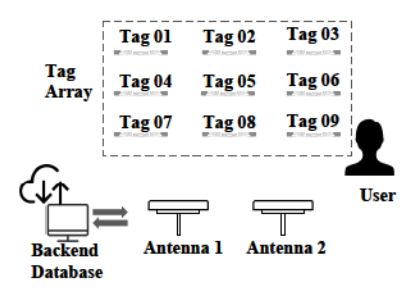


Fig. 10. Setup of an example

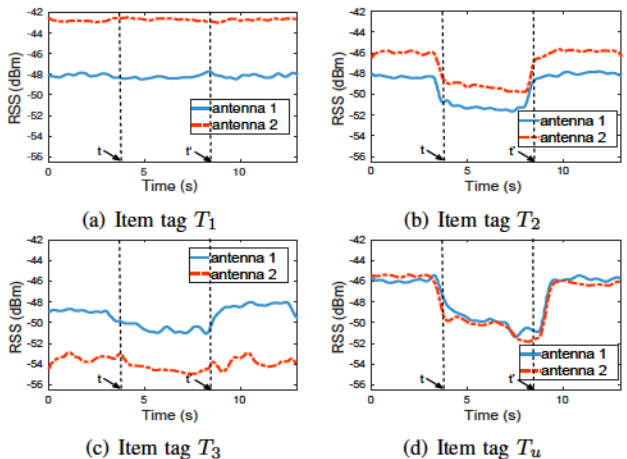


Fig. 11. RSS profiles of item tags and user tag acquired by 2 antennas

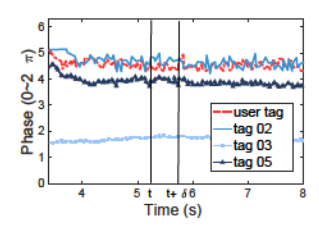


Fig. 12. Phase difference profile of four tags

TagMii first gets current phase difference profiles $D^1, D^2...D^n$ for n candidate tags, where D^i is tag i's phase difference profile in time interval (t, t+T). After interpolation in Section IV-B, these n vectors should have equal length, which we denote as L.

TagMii then calculates the Euclidean distance between the phase difference profile vectors of user tag u and each candidate item tag i,

$$L^{i} = \sqrt{\sum_{k=1}^{L} (e_{k}^{i} - e_{k}^{u})^{2}}$$
 (10)

where e_k^i and e_k^u are the k-th elements of the phase difference profile D^i and D^u , respectively. TagMii performs calculations between user tag u and every candidate tag, and then finds the item tag i whose L^i satisfies $|L^i-L^u| \leq L_h$ and records the top M tags that has the least L^i values from them, which are most likely in the coupling state with user tag. L_h is a empirically pre-defined threshold for comparison. After choosing the top M tags, TagMii uses a $N_c \times T_l$ matrix V to records the comparison result. The one with the smallest L_i will be assigned with 1 and the second one with 2 and so on.

Hence, each element (i,t) in V represents the tag i's result in the top M list at t-th segment (V(i,t)=0 if i is not in the list). For example, if the element V(3,2) is 1, it indicates that tag 3's has the highest similarity with the user tag in 2-th profile segment.

After finding the candidate tag that minimizes the distance, we can obtain an array V for all T_l segments. Our goal is to determine the tag with the most occurrences of 1 in V, which is most likely the one coupling with the user tag.

In the example shown in Fig. 10, the user is interaction with Tag 2 among all nine item tags. The RSS profiles of the tags around Tag 2 as well as the user tag are shown in Fig. 11. After candidate tag selection, three tags are selected as the *candidate tags*, namely Tags 2, 3, and 5. The phase different profiles of three candidate tags and the user tag are shown in Fig. 12. Although all three candidate tags have signal changes caused by the user movement, TagMii is still able to select Tag 2 as the interacting tag by analyzing the phase profile.

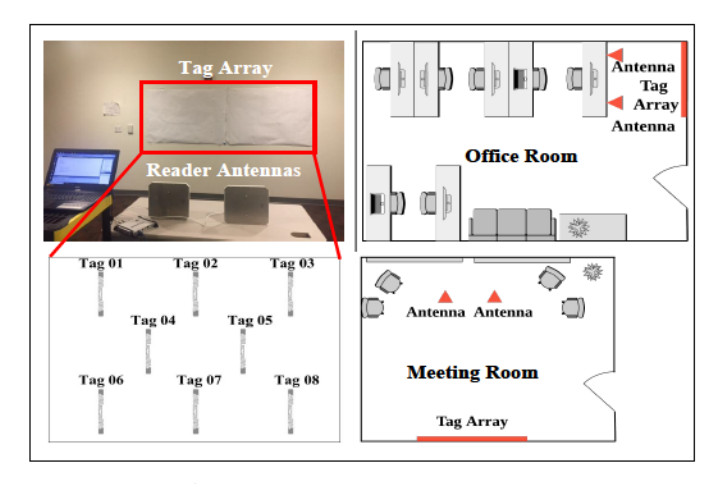
V. IMPLEMENTATION AND EVALUATION

A. Prototype Implementation

We build a TagMii prototype based on COTS UHF RIFD devices: an ImpinJ Speedway modeled R420 RFID reader, two Laird S9028-PCL directional antennas, and three models of tags: ALN-9740, ImpinJ E41C/B, and Alien 964X. We observed inductive coupling for all models of tags. Even if two tags are in different models, inductive coupling still occurs and can be recognized by TagMii. In fact, as long as one model of tags work, TagMii can be successfully implemented and used. We only show the results of using ImpinJ E41C/B. Each item for evaluation is attached with an ImpinJ E41C/B tag. We deploy the reader antennas in a distance about 2m away from the tag array. Note one reader may connect to multiple antennas and the antennas are not necessarily at the same location of the reader - depending on the length of the cable. Hence one reader is sufficient to cover a large indoor area. The transmission gain and receiving gain are both 25dB. The prototype is compatible to the standard EPC Class 1 Generation 2 protocols(C1G2). We run the software components of TagMii at a Dell desktop, equipped with Intel Core i7-7700 CPU at 3.6GHz and 16G memory.

B. Evaluation Methodology

We evaluate the performance of TagMii in two complex environments with various multipath reflectors, moving objects, wireless signals (WiFi, LTE, and Bluetooth), electrical devices (servers, workstations, printers, refrigerator), and magnetic fields (whiteboard): (a) an office room and (b) a meeting room as shown in Fig. 13(a). The office environment simulates a retail store where shelves are densely placed, and the meeting room simulates the museum application where artworks are placed on the wall. In office environment we use a tag array that is with 3 rows and 5 columns as illustrated in Fig.13(a) to simulate the tags attached on a rack of commodities or exhibitions, while in the meeting room we further exploit TagMii's performance when tags are attached



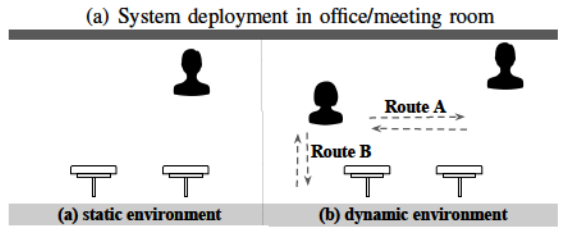


Fig. 13. Different environments

in a line. The location of the tag array is highlighted with red markers shown in Fig.13(a)

To be consistent with the real implementation, the distance between the reader antennas and the tag array is 1.5m in office room and 3m in meeting room. Note in practice reader antennas can be hung from the ceiling to reduce the probability of blocking LOS signals by moving objects. Note although in theory UHF RFID can operate in 10m distance, practical deployments usually only allow the distance to be around 3m or less. However we are not able to reconstruct the ceiling to hang antennas. The distance between two adjacent tags is initially set to be 30cm in the office room and 80cm in meeting room, while the horizontal distance between them are both set to be 30cm. We will show that longer distance between adjacent tags will result in more accurate results. Consider the application in retail stores, it will be rather time- and cost-inefficient if each item is attached with a passive tag. Moreover, a large tag population will degrade the sampling rate for each tag. We may assign one item tag for each type of items. Hence 30cm distance is a practical setting. In our experiments, we invite 4 volunteers with heights varying from 160cm to 180cm. We let volunteer arbitrarily move in the space and use their tags to interact with the item tags in the environment. In the worst case, a moving volunteer may block the LOS path of the signal between tags and the reader antenna as shown in Fig.13. Each user is only trained with 3 minutes on what they should do to interact with item tags.

Every accuracy value shown in this section is the average of 120 production experiments.

In the following subsections, we will first show the evaluation results of two important steps of TagMii respectively, namely interaction event detection and coupling tag determi-

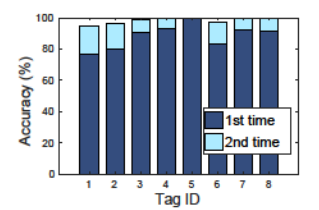


Fig. 14. Detection accuracy in 1st and 2nd time

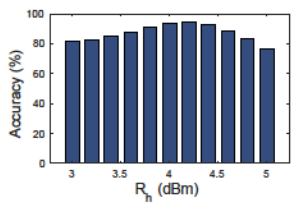


Fig. 15. 1st-time accuracy vs. R_h

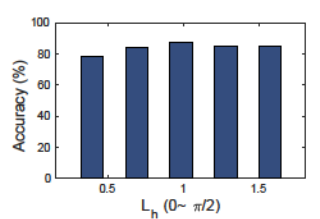


Fig. 16. Impact of threshold L_h

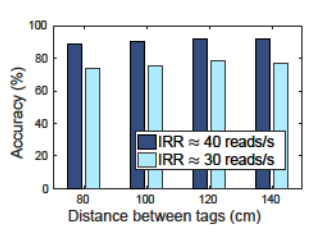


Fig. 17. Accuracy with smaller IRR

nation.

C. Interaction Event Detection

Evaluation metrics. The interaction event detection step reports the events of interactions. We use two metrics to evaluate the accuracy of this step: 1) Among all interaction events performed by the users, the *accuracy* is defined as the ratio of events that are successfully detected by TagMii. 2) We also let a user carry a user tag, walk in front of the item tag array, but do not perform any tag interaction. The *false detection rate* is the number of interaction events reported, which did not actually happen, during a given time period.

Fig. 14 shows the accuracy for the 1st-time action and the improvement of a 2nd-time action. If an interaction fails to be detected by TagMii for the 1st time, repeating the interaction for a 2nd time may possible success, similar to the user experience of most input interfaces. The detection accuracy for all 8 tags in the environment can be >95% for two-time actions. As discussed in Sec. IV-A, TagMii uses a pre-defined threshold R_h to detect interaction events. We vary R_h from 3dBm to 5dBm with a step of 0.2dBm and record the accuracy change of interaction detection. As shown in Fig. 15, TagMii achieves a best 1st-time accuracy when the R_h is 4.2dBm. Using other setups, the best-case thresholds are similar. Hence we use this threshold value in the following experiments.

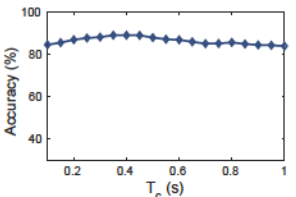
In this set of experiments, we ask four volunteers to carry the user tags and walk in front of the tag array without interacting with any item tag. The false positive rate is measured in number of false positives per minute (FPPM). We vary the distance between the user to the tag array in four different values from 40cm to 100cm. In each experiment we ask each user to walk for 1.5 minutes. We repeat the experiment for four users and two different walk speeds. The results are shown in Table I. The values 0.17 and 0.33 are all in FPPM. Hence the chance of false positives is very small.

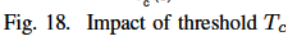
D. Target Tag Determination

Evaluation metric. The accuracy μ of the target tag determination step is defined as: $\mu = n_p/n_o$, where n_o is

	Distance (cm)				
Walking Speed (m/s)	40	60	80	100	
0.75	0.17	0.17	0	0	
1.5	0.33	0	0.17	0	

TABLE I FALSE POSITIVES PER MINUTE





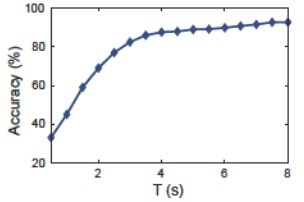


Fig. 19. Impact of window size T

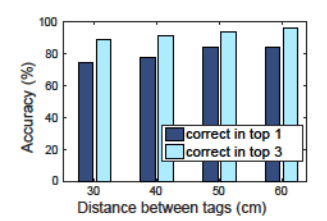


Fig. 20. Impact of distance between item tags (office)

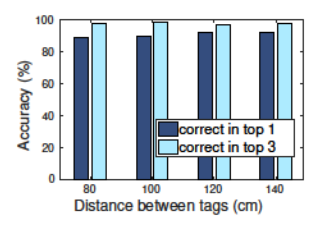


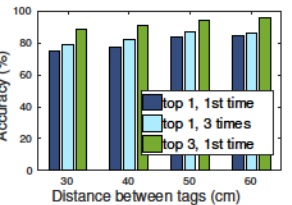
Fig. 21. Impact of distance between item tags (meeting room)

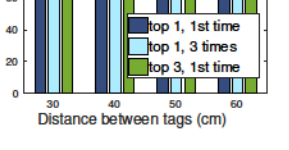
the total number of interaction operations performed by the users, and n_p is the number of tag pairs that are correctly determined as coupling tags among them.

Impact of threshold L_h : The comparison threshold L_h plays a important role in judging whether a tag can be considered as a choice in top list. Intuitively, if L_h is too large, then the system may probably take many irrelative item tags into consideration. On the contrary, a small L_h may cause the miss of target item tag. We vary L_h from 0 to $\frac{\pi}{2}$, and show the accuracy μ of TagMii in Fig. 16. TagMii can maintain an accuracy of about 88% when $L_h = \pi/4$ and this value is consistency across different setups, hence we set the comparison threshold to be $\pi/4$.

Impact of threshold T_c : If the time interval threshold T_c too large, TagMii will select too many item tags as candidate tags. Also a small T_c might cause not including the target item tag as a candidate. We vary T_c from 0.1s to 1s, and show the accuracy μ of TagMii in Fig. 18. The accuracy of TagMii is relatively stable by varying T_c , but it still achieves a relative high value when $T_c = 0.4$ s. We use this threshold value in the other experiments.

Operation duration T: As mentioned in Section IV-D, we use a filter with sliding window to process the collected data. Intuitively a longer operation duration T for user to put its user tag close to the item tag will result in higher accuracy. However, the user experience will downgrade if the operation lasts very long. We vary the time window size T from 0.5s to 8s and show the accuracy in Fig. 19. It shows that when T=4s, the accuracy of TagMii can stay in a high value for all experimental scenarios. Hence, TagMii requires each user to put the user tag for 4s in the other experiments. Note that a user may receive feedback earlier than 4s.





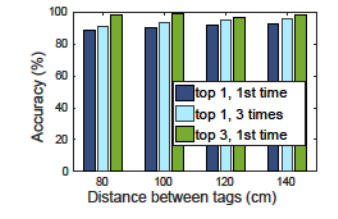


Fig. 22. Accuracy with retrying (of-

Fig. 23. Accuracy with retrying

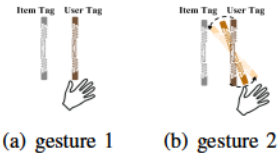








Fig. 24. Differen gestures

E. Overall Performance of TagMii

We evaluate the performance of TagMii in the static environments where there is only one user interacting with the items (Fig. 13a) and in dynamic environments where moving people exist (Fig. 13b). The accuracy of TagMii is defined as the ratio of correctly recognizing the two tags involved in each interaction event. In addition, we also show the accuracy of recognizing the tags with up to two repeated interaction actions, if TagMii reports no result to the 1st-time action. Note if TagMii reports a wrong result, then this experiment will be considered failed immediately. We denote this as the accuracy in 3 times. Also we are interested in explore if the target tag is in the top-3 list of candidates of TagMii, if it is not top 1. Some human-computer interaction applications support the following function: if the system is hard to select the most relevant target, it can show the top-3 list and let the user to select the correct one. We denote this as the accuracy in top-3 list.

Impact of distance between item tags. We conduct the experiments by varying the distance between the item tags from 30cm to 60cm in the office and from 80cm to 120cm in the meeting room. The results are shown in Fig. 20 and Fig. 21. We find that for single user case, the accuracy of top 1 results is higher than 75% even if $d_t \approx 30cm$, a very dense placement setup. When we increase the distance, the accuracy of TagMii significantly increase. For distance > 1m, the accuracy of top 1 and top 3 results are around 90% and 98% respectively.

Accuracy with retrying. From the experiments in Fig. 20 we notice that there are two types of failures in TagMii. One is the that TagMii reports no result and the other is that TagMii reports a wrong result. In the no-result cases, we further explore if one or two extra retrying will give a correct result. We show the accuracy in 3 times in Figs. 22 and 23. We find retrying does improves the accuracy though not in a big margin.

Impact of different coupling gestures. We also evaluate the performance of TagMii when the user tag is not placed correctly. We ask the user to rotate the tag (Fig.24(b)), to move the tag up and down (Fig. 24(c)), or to move the tag around

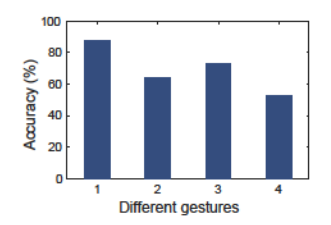


Fig. 25. Impact of different reading gestures

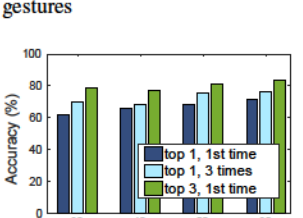


Fig. 27. Accuracy with route A (office room)

Distance between tags (cm)

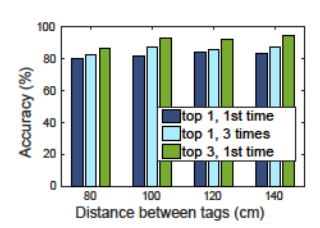


Fig. 29. Performance of route B in meeting room

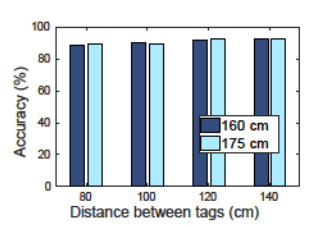


Fig. 26. Impact of different users' heights

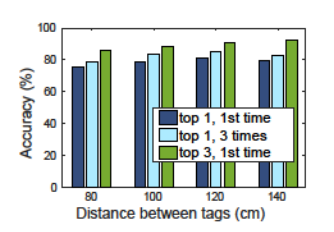


Fig. 28. Accuracy with route A (meeting room)

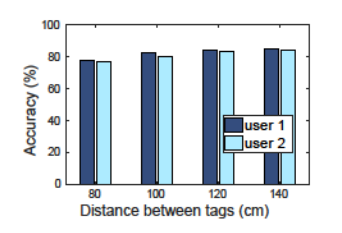


Fig. 30. Accuracy for concurrent users

the item tag(Fig.24(d)). We show the corresponding accuracy in Fig.25. All incorrect gestures will lower the accuracy, but the accuracy is always > 50%.

Impact of moving people. While conducting the experiments, we ask one extra volunteer to talk around the reader antennas with two patterns shown in Fig. 13(b). Route A will block the LOF signals. Route B does not but still makes the RFID signal more complicated. Comparing Fig. 27 with Fig. 22 and Fig. 23 with Fig. 28, we find that Route A could possibly lower the accuracy of TagMii by 10% to 15%. Route B provides better results as shown in Fig. 29.

Processing time. We show the processing time of TagMii to determine the interacting tags in Table II. We vary the distance between two item tags from 40cm to 120cm. The results show that the processing time of TagMii is very short (< 1sec) for all experiments.

Concurrent interactions. We study the case that two users concurrently interact with their target item tags. TagMii should be able to recognize which user tag pairs to which item tag. The results in Fig. 30 shows the accuracy of the two users respectively. Compared to the single-user case, the accuracy is reduced by 10%. However it still maintains in a high level.

Distance (cm)	40	60	80	100	120
Time (sec)	0.7696	0.7364	0.8189	0.7972	0.7783

TABLE II AVERAGE PROCESSING TIME

VI. DISCUSSION

The current RFID protocol uses slotted ALOHA as the MAC layer solution. Hence tags competes the time slots to reply to the reader. The commodity RFID readers support a constant number of successful read operations per second (around 400 on our device), regardless of the number of tags with the interrogate range. When the number of tags increases, the share of time slots of every tag decreases. We define *individual reading rate* (IRR) as the number of readings obtained from a particular tag per second [42]. In order to achieve high accuracy, the IRR of a tag should be sufficiently high, such that its state changes can be continuously and correctly captured. Missing RSS and phase samples will consequently reduce the accuracy of both candidate tag selection and coupling tag determination.

Fig. 23 shows an example in which eight items and four users are tagged. In this set of experiments we further attach five more tags in the environment without any other changes on experiment settings. Consequently, the average IRR of each tag reduces from about 40 reads/sec to fewer than 30 reads/sec.Fig. 17 shows that lower IRR will result in obvious accuracy decrease. We leverages several possible methods to improve the IRR, including: (1) Decrease EPC length. Shorter packet durations can increase the individual reading rate. One approach is to decrease the Electronic Product Code (EPC) length. Following the commercial EPC C1G2 standard, the length of EPC code can be set to 8-bit at a minimum [1]. We may adopt this length in our implementation. (2) Adopt FM0 reader inventory mode. As another approach to decrease packet lengths, the reader may use faster reader inventory mode (i.e., FM0 mode) to speed up the communication rate [16]. (3) Utilize PHY-layer filtering. The PHY-layer filtering feature is supported by the RFID Class 1 Generation 2 (C1G2) protocol, which allows the reader to read only a subsection of the tags [42].

VII. CONCLUSION

TagMii is a new approach to enable user-item interactions using passive RFID tags. Compared to other solutions that require a user to carry non-trivial hardware, TagMii only requires every user to carry a passive tag. The reader deployed in the environment monitors the interaction events and pair the user tag and the corresponding item tag. The key advantage of TagMii is that it is cost-efficient and especially convenient for children, some seniors, people with certain disabilities, and others who do not operate smartphones. We evaluate TagMii in complex environments with rich multipath, mobility, wireless signals, and magnetic fields and find TagMii to be accurate in recognizing user-item interactions in various setups.

VIII. ACKNOWLEDGEMENT

This work is partially supported by National Science Foundation Grant 1717948 and 1750704. We thank the anonymous reviewers for their suggestions and comments.

REFERENCES

- EPC Global. Specification for RFID Air Interface EPC[™] Radio-Frequency Identity Protocols Class-1 Generation-2 UHF RFID Protocol for Communications at 860 MHz-960 MHz. Technical report, Technical report, GS1, 2008.
- [2] M. Kodialam and T. Nandagopal. Fast and Reliable Estimation Schemes in RFID Systems. In *Proc. of ACM MOBICOM*, 2006.
- [3] C. Qian, H. Ngan, Y. Liu, and L. M. Ni. Cardinality Estimation for Large-scale RFID Systems. *IEEE Transactions on Parallel and Distributed Systems*, 2011.
- [4] Z. Zhou, B. Chen, and H. Yu. Understanding RFID Counting Protocols. IEEE/ACM Transactions on Networking, 2016.
- Yiyang Zhao, Yunhao Liu, and Lionel M. Ni. VIRE: Active RFID-based Localization Using Vrtual Reference Elimination. In *Proceedings of IEEE ICPP*, 2007.
- [6] Xiaofeng Shi, Minmei Wang, Ge Wang, Baiwen Huang, Haofan Cai, Junjie Xie, and Chen Qian. TagAttention: Mobile Object Tracing without Object Appearance Information by Vision-RFID Fusion. In *Proceedings* of IEEE ICNP, 2019.
- [7] Lionel M. Ni, Yunhao Liu, Yiu Cho Lau, and Abhishek P. Patil. LANDMARC: Indoor Location Sensing Using Active RFID. Wireless Networks, 10(6):701–710, 2004.
- [8] Cory Hekimian-Williams, Brandon Grant, Xiuwen Liu, Zhenghao Zhang, and Piyush Kumar. Accurate Localization of RFID Tags Using Phase Difference. In *Proceedings of IEEE RFID*, 2010.
- [9] Tianci Liu, Lei Yang, Qiongzheng Lin, Yi Guo, and Yunhao Liu. Anchor-free Backscatter Positioning for RFID Tags with High Accuracy. In Proceedings of IEEE INFOCOM, 2014.
- [10] Lei Yang, Yekui Chen, Xiang-Yang Li, Chaowei Xiao, Mo Li, and Yunhao Liu. Tagoram: Real-time Tracking of Mobile RFID Tags to High Precision Using COTS Devices. In Proceedings of the 20th annual international conference on Mobile computing and networking, pages 237–248. ACM, 2014.
- [11] Longfei Shangguan, Zhenjiang Li, Zheng Yang, Mo Li, and Yunhao Liu. OTrack: Order Tracking for Luggage in Mobile RFID Systems. In Proceedings of IEEE INFOCOM, 2013.
- [12] Longfei Shangguan, Zheng Yang, Alex X. Liu, Zimu Zhou, and Yunhao Liu. Relative Localization of RFID Tags Using Spatial-Temporal Phase Profiling. In *Proceedings of USENIX NSDI*, 2015.
- [13] Lei Yang, Qiongzheng Lin, Xiangyang Li, Tianci Liu, and Yunhao Liu. See Through Walls with COTS RFID System! In *Proceedings of ACM MOBICOM*, 2015.
- [14] Jinsong Han, Chen Qian, Xing Wang, Dan Ma, Jizhong Zhao, Wei Xi, Zhiping Jiang, and Zhi Wang. Twins: Device-free Object Tracking Using Passive Tags. *IEEE/ACM Transactions on Networking (TON)*, 24(3):1605–1617, 2016.
- [15] Yunfei Ma, Nicholas Selby, and Fadel Adib. Minding the Billions: Ultrawideband Localization for Deployed RFID Tags. In *Proceedings of ACM Mobicom*, 2017.
- [16] Jinsong Han, Han Ding, Chen Qian, Dan Ma, Wei Xi, Zhi Wang, Zhiping Jiang, and Longfei Shangguan. CBID: A Customer Behavior Identification System Using Passive Tags. In *Proceedings of IEEE ICNP*, 2014.
- [17] Longfei Shangguan, Zimu Zhou, Xiaolong Zheng, Lei Yang, Yunhao Liu, and Jinsong Han. Shopminer: Mining Customer Shopping Behavior in Physical Clothing Stores with COTS RFID Devices. In *Proceedings* of ACM SenSys, 2015.
- [18] Han Ding, Chen Qian, Jinsong Han, Ge Wang, Wei Xi, Kun Zhao, and Jizhong Zhao. RFIPad: Enabling Cost-efficient and Device-free In-air Handwriting Using Passive Tags. In *Proceedings of IEEE ICDCS*, 2017.
- [19] Lei Yang, Yao Li, Qiongzheng Lin, Xiang-Yang Li, and Yunhao Liu. Making Sense of Mechanical Vibration Period with Sub-millisecond Accuracy Using Backscatter Signals. In *Proceedings of ACM Mobicom*, 2016.
- [20] Phychips Inc. http://www.phychips.com/applications-main/.
- [21] ImpinJ Inc. http://www.impinj.com/.
- [22] Zhenlin An, Qiongzheng Lin, and Lei Yang. Cross-Frequency Communication: Near-Field Identification of UHF RFIDs with WiFi! In Proceedings of the 24th Annual International Conference on Mobile Computing and Networking, pages 623–638. ACM, 2018.
- [23] CL Turner, AC Casbard, and MF Murphy. Barcode Technology: Its Role in Increasing the Safety of Blood Transfusion. *Transfusion*, 43(9):1200– 1209, 2003.

- [24] Trupti Lotlikar, Rohan Kankapurkar, Anand Parekar, and Akshay Mohite. Comparative Study of Barcode, QR-code and RFID System. Int. J. Comput. Technol. Appl., 4(5):817–821, 2013.
- [25] Yong Ming Kow, Xinning Gui, and Waikuen Cheng. Special Digital Monies: The Design of Alipay and Wechat Wallet for Mobile Payment Practices in China. In *IFIP Conference on Human-Computer Interaction*, pages 136–155. Springer, 2017.
- [26] Mabel Vazquez-Briseno, Francisco I Hirata, Juan de Dios Sanchez-Lopez, Elitania Jimenez-Garcia, Christian Navarro-Cota, and Juan Ivan Nieto-Hipolito. Using RFID/NFC and QR-code in Mobile Phones to Link the Physical and the Digital World. In *Interactive Multimedia*. IntechOpen, 2012.
- [27] Parvin Asadzadeh, Lars Kulik, and Egemen Tanin. Gesture recognition using rfid technology. *Personal and Ubiquitous Computing*, 16(3):225– 234, 2012.
- [28] Jue Wang, Deepak Vasisht, and Dina Katabi. Rf-idraw: Virtual touch screen in the air using rf signals. In ACM SIGCOMM Computer Communication Review, volume 44, pages 235–246. ACM, 2014.
- [29] Hanchuan Li, Can Ye, and Alanson P Sample. Idsense: A human object interaction detection system based on passive uhf rfid. In *Proceedings* of the 33rd Annual ACM Conference on Human Factors in Computing Systems, pages 2555–2564. ACM, 2015.
- [30] Hanchuan Li, Eric Brockmeyer, Elizabeth J Carter, Josh Fromm, Scott E Hudson, Shwetak N Patel, and Alanson Sample. Paperid: A technique for drawing functional battery-free wireless interfaces on paper. In Proceedings of the 2016 CHI Conference on Human Factors in Computing Systems, pages 5885–5896. ACM, 2016.
- [31] Swadhin Pradhan, Eugene Chai, Karthikeyan Sundaresan, Lili Qiu, Mohammad A Khojastepour, and Sampath Rangarajan. RIO: A Pervasive RFID-based Touch Gesture Interface. In Proceedings of the 23rd Annual International Conference on Mobile Computing and Networking, pages 261–274. ACM, 2017.
- [32] Yuri Álvarez López, María Elena de Cos Gómez, and Fernando Las-Heras Andrés. A received signal strength rfid-based indoor location system. Sensors and Actuators A: Physical, 255:118–133, 2017.
- [33] Kirti Chawla, Christopher McFarland, Gabriel Robins, and Connor Shope. Real-time rfid localization using rss. In 2013 International Conference on Localization and GNSS (ICL-GNSS), pages 1–6. IEEE, 2013.
- [34] Longfei Shangguan, Zheng Yang, Alex X Liu, Zimu Zhou, and Yunhao Liu. Stpp: Spatial-temporal phase profiling-based method for relative rfid tag localization. *IEEE/ACM Transactions on Networking*, 25(1):596– 609, 2016.
- [35] Chengkun Jiang, Yuan He, Xiaolong Zheng, and Yunhao Liu. Orientation-aware rfid tracking with centimeter-level accuracy. In Proceedings of the 17th ACM/IEEE International Conference on Information Processing in Sensor Networks, pages 290–301. IEEE Press, 2018
- [36] Jue Wang and Dina Katabi. Dude, where's my card?: Rfid positioning that works with multipath and non-line of sight. In ACM SIGCOMM Computer Communication Review, volume 43, pages 51–62. ACM, 2013.
- [37] Han Ding, Jinsong Han, Chen Qian, Fu Xiao, Ge Wang, Nan Yang, Wei Xi, and Jian Xiao. Trio: Utilizing tag interference for refined localization of passive rfid. In *IEEE INFOCOM 2018-IEEE Conference on Computer Communications*, pages 828–836. IEEE, 2018.
- [38] Jae Sung Choi, Hyun Lee, Daniel W Engels, and Ramez Elmasri. Passive uhf rfid-based localization using detection of tag interference on smart shelf. IEEE Transactions on Systems, Man, and Cybernetics, Part C (Applications and Reviews), 42(2):268–275, 2011.
- [39] Ge Wang, Haofan Cai, Chen Qian, Jinsong Han, Xin Li, Han Ding, and Jizhong Zhao. Towards replay-resilient rfid authentication. In Proceedings of the 24th Annual International Conference on Mobile Computing and Networking, pages 385–399, 2018.
- [40] Ge Wang, Chen Qian, Jinsong Han, Wei Xi, Han Ding, Zhiping Jiang, and Jizhong Zhao. Verifiable Smart Packaging with Passive RFID. In Proceedings of ACM UBICOMP, 2016.
- [41] EPCglobal Ratified Standard. Epct m radio-frequency identity protocols class-1 generation-2 uhf rfid protocol for communications at 860mhz-960mhz version 1.0. 9, 2005.
- [42] Qiongzheng Lin, Lei Yang, Chunhui Duan, and Yunhao Liu. Revisiting reading rate with mobility: Rate-adaptive reading of cots rfid systems. *IEEE Transactions on Mobile Computing*, 18(7):1631–1646, 2018.